A Practical UWB Microwave Imaging System Using Time-Domain DORT for Tumor Detection

S. Sadeghi and R. Faraji-Dana

School of Electrical and Computer Engineering, College of Engineering
University of Tehran, Tehran, Iran
sajjadsadeqi@ut.ac.ir, reza@ut.ac.ir

Abstract ─ In this paper Time Reversal (TR) and Decomposition of Time Reversal operator (DORT) methods are employed in an Ultra-WideBand (UWB) microwave imaging system. The possibility of multiple tumor detection in using selective focusing DORT is investigated and a number of improvements are proposed in DORT algorithm. A practical UWB imaging system for tumor-like object detection consisting of just two revolving UWB antennas is then introduced. The proposed system does not need costly switches or network analyzers as it just uses a UWB transceiver to acquire the required time domain signals. Challenging problems of this system are addressed and their solutions are proposed and vindicated through both simulations and measurements carried out on a simple model by using an experimental setup. The proposed system is suitable for different applications such as breast cancer and tumor detection where high accuracy and resolution is necessary.

Index Terms ─ DORT and tumor detection, microwave imaging, time-reversal.

I. INTRODUCTION

In recent years, microwave imaging has gained diverse applications in different domains such as radar imaging [1,2], detection of buried objects [3], detection of fault in networks [4], medical imaging [4–8], and so on. Among these applications, early detection and localization of breast cancer tumors has obtained considerable attention. Several algorithms have already been introduced for the improvement of accuracy and obtaining a better resolution of the detection [7–12]. This growing attention is especially motivated by the significant contrast in the dielectric properties of malignant breast tissues and the background medium at microwave frequencies.

Microwave imaging methods for tumor detection is mainly divided in two different categories: tomography imaging and ultra-wideband (UWB) radar imaging. In tomography imaging, dielectric properties of tissue are obtained by solving an inverse scattering problem. In contrast, in UWB radar imaging the goal is to identify and localize significant scatterers in the tissues. As a result, a much simpler problem has to be solved compared to the former category.

Among different methods proposed in UWB imaging, the time-reversal (TR) methods which were first developed and implemented in acoustics [13], show a better performance in high clutter and noisy environments like breast tissues [14].

Conventional TR methods can only detect the dominant scatterer; thus, no information about other scatterers would be achieved. In order to overcome this shortcoming, eigenvalue decomposition (EVD) of the time-reversal operator (TRO) is employed [14]. The eigenvalues and related eigenvectors of the TRO provide the required information about all well-resolved point-like scatterers. Using these eigenvectors and transmitting them by the detecting antenna array makes selective focusing of each scatterer possible. This strategy is the basis of the decomposition of the time-reversal operator (DORT) method [15].

In most of the previous work, DORT method is used in single or multiple frequency schemes while some major challenges would occur when employing DORT in UWB imaging systems. In UWB DORT, first the EVD is applied on several discrete frequencies in the desired frequency range, next discrete time domain signal is obtained by using inverse discrete Fourier transform (IDFT) [14]. In this process the main challenge is how to relate different eigenvalues to distinct scatterers in the frequency range. To the best of our knowledge this problem which results in the loss of information of some scatterers has not been properly addressed in the literature. In this paper, we propose a new method to overcome this problem through sorting the eigenvalues at each frequency.

Another challenge arises from the lack of knowledge about the frequency dependence of the phases of eigenvectors. In fact, no information exists on the phases of the frequency domain signals. Therefore, after performing the IDFT the time domain results become incoherent. This is particularly important in

inhomogeneous background media with multiple scatterers, where multiple reflections has to be coherently combined over the entire bandwidth at the target(s) location(s) [16]. Such preprocessing can be done by using a power singular value decomposition (SVD) or by projecting the incoherent eigenvectors onto columns of the MDM [16, 17]. In [16], space-frequency TR is used for UWB imaging. In this paper however we introduce a new modification in the phase of eigenvectors to achieve coherent time-domain signals.

By addressing the above-mentioned challenges in employing DORT in a practical UWB imaging system, we built and employed an imaging system for breast cancer detection at the UWB frequency band of 3.1-10.6 GHz. This system uses two moving antennas for transmitting and receiving signals. This arrangement is much simpler and less-expensive compared with the previously introduced complicated systems [18-22] and will be shown to enjoy comparable performance.

This paper is organized as follows. In Section II the conventional TR method along with some improving modifications are introduced. The proposed microwave imaging system is presented in Section III. Validating system performance through simulations and measurements will be given in Sections IV and V, respectively. Section VI concludes the paper.

II. TIME REVERSAL METHOD

Time reversing is the retransmission of the received electromagnetic waves in the receivers back to the propagation medium in the reverse form relative to time. In this method the received signals in the receivers are first reversed and then transmitted back into the medium. It can be shown that these transmitted signals will propagate back in the same paths as in the forward propagation and focus on near to the primary source in practical situation [23]. This behavior of the reversed waves remains true in a situation where the medium contains unknown scatterers imposing reflection, refraction or diffraction on the propagating waves.

In media with multiple discrete scatterers, back-propagation of the time reversed scattered fields, causes the focal spots to be created on all scatterers at the same time, naturally with more intensity expected on the dominant scatterer. As a result, the information of dominated scatterers may be lost. In DORT, this problem is overcome by isolating and sorting different scatterers by using eigenvalue decomposition.

In DORT method, N transceiver antennas, called time-reversal array (TRA), generate an N×N symmetric matrix denoted by $K(t)$. This symmetry is due to the reciprocity property of the electromagnetic fields. In the frequency domain this matrix is represented by $K(\omega)$ and is referred to as the Multi Data Matrix (MDM), where ω is the angular frequency [14]. TR operation in

the time domain corresponds to the phase conjugation in the frequency domain denoted by the Hermitian conjugate $K^{\dagger}(\omega)$. In [14], TRO is defined as the self-adjoint matrix of $T(\omega) = K^{\dagger}(\omega)K(\omega)$. By applying singular value decomposition (SVD) to $K(\omega)$, it is given by $K(\omega) = U(\omega)\Lambda(\omega)V^{\dagger}(\omega)$, where is the diagonal matrix of singular values and $U(\omega)$ and $V(\omega)$ are unitary matrices. In this way the EVD of the TRO can be written as $T(\omega) = V(\omega)S(\omega)V^{\dagger}(\omega)$, where $S(\omega) = \Lambda^{\dagger}(\omega)\Lambda(\omega)$ is the diagonal matrix of eigenvalues [14]. It is obvious that the eigenvalues of the TRO and the squared singular values of the MDM are equal; hence, both expressions are used interchangeably in references.

Normalized eigenvectors of the TRO form the columns of the unitary matrix $V(\omega)$ [24]. In the case of recognizable point-like scatterers in homogeneous media, each significant eigenvalue of the TRO means a single scatterer generating isotropic scattered fields. Since in reality no scatterer generates isotropic EM waves multiple eigenvalues will be referring to a single scatterer [25, 26]. In this case, the associated eigenvector $v_p(\omega_c)$, where ω_c is the central operation frequency, produces the back-propagated fields radiated from the TRA for focusing on the pth scatterer. The normalized vector $v_p(\omega_c)$ is the pth column of $V(\omega_c)$. However, a similar decomposition should be applied to the entire bandwidth at each frequency point to make a frequency dependent amplitude distribution of eigenvectors for UWB signals.

The main difficulty of this algorithm lies in the fact that locating and tracking of singular values in the frequency domain is a challenge due to the change of their orders. In Fig. 1 singular values of a sample configuration consisting of two PEC spheres with two different radii r1=1.5 cm and r2=0.5 cm are shown. As it is clear in the figure, due to the comparable sizes of the scatterers with the wavelengths of the frequency components of a UWB signal, there exist multiple singular values with considerable magnitudes in the entire frequency band. Also, changes in the order of singular values at different frequencies are evident as marked by arrows in the figure.

In our implementation of the DORT in a UWB system, we solved this problem by using the orthogonality of eigenvectors. It is obvious that at a single frequency, eigenvectors of a specific scatterer are parallel and eigenvectors of two well-resolved scatterer are orthogonal. By tracking the inner product of dominant eigenvectors in adjacent frequencies, eigenvectors of each scatterer in the entire frequency band will be identified. In Fig. 2 inner product of the two first eigenvectors in the imaging problem of Fig. 1 is

shown. As it is seen the inner product of the 1st and 2nd eigenvectors are almost zero while and self-inner product of the 1st eigenvectors are almost equal to 1. Also, for the eigenvalues whose orders have been changed inner products of the 1st and 2nd eigenvectors are greater than self-inner product. It is evident that by using this technique eigenvalues and eigenvectors which have changed their order can be identified.
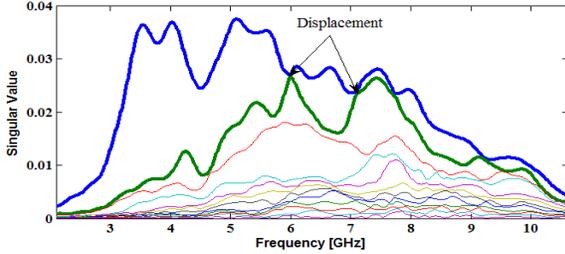

Fig. 1. Variations of singular values of two PEC spheres with different radii over the entire UWB frequency band.
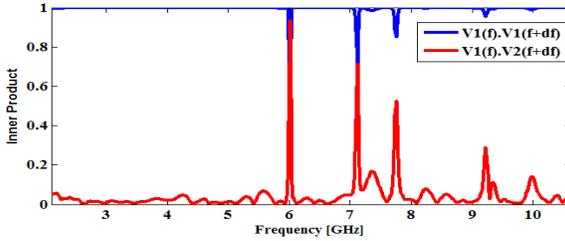

Fig. 2. Inner product of the 1st eigenvector by itself (blue), and the 1st and 2nd eigenvectors (green), in two adjacent frequencies.

The second challenging problem in using the frequency domain eigenvectors in image reconstruction process is the lack of knowledge about the true relative phases of eigenvectors. In [16], left singular vectors of TRO is obtained by using:

$$u_p(\omega) = e^{j\Phi_{SVD}(\omega)} \frac{g(\overline{X_p},\omega)}{\left\| g^*(\overline{X_p},\omega) \right\|}, \qquad (1)$$

where u_p is the pth left singular vector, $\Phi_{SVD}(\omega)$ is the frequency-dependent phase of SVD, g is Green's function vectors which relates the scatterer location to TRA and finally $\overline{X_p}$ is the location of the pth scatterer in medium.

One may find other methods like space frequency TR [16], [27] or phase smoothing [14] to overcome this problem. In this paper we propose a simple solution to this problem. Since in computing the eigenvectors with MATLAB the first element of each vector has a random phase and the phases of all other elements are determined relative to the first element, we have set the phase of first element to zero while preserving the relative phases of

other elements. With this modification a coherent signal could be obtained. Also, since the eigenvectors are normalized to 1, these vectors need to renormalize to their corresponding eigenvalues. In the TR process these vectors have to be conjugated as well. These operations can be written as $(\lambda_p u_p)^* = \lambda_p u_p^* = \lambda_p v_p$, and the time-domain signals are calculated by using the inverse Fourier transform $e_p(t) = F^{-1}\{\lambda_p(\omega)v_p(\omega))\}$.

After reconstructing the required time domain signals for back-propagation by following the above-mentioned procedure, the last step is the retransmitting of the signals by TRA to the medium. For retransmitting of the signals, solving a forward problem by using the excitation signal $e_p(t)$ at the transmitters is required. In solving this forward problem, electric field at each time step at all positions should be computed and saved. Then by assigning a color map to the field strength at each position, the image at that time will be constructed.

The last issue arises in the construction of final images by the TR method is the selection of optimum time when the waves converge to the scatterers. The images in this time have an intense peak at the object locations and lower intensity at other locations. Since these images have a small entropy, minimum entropy can be used as a criterion for selecting optimum time images. In [28] the inverse of varimax norm is used for the computation of entropy. This criterion has also been used for breast cancer detection in [28, 30]. It reads as:

$$R(E_{tot}^{n\,2}) = \frac{\left[\sum_{j,k}\sum E_{tot}^{n\,2}(j,k)\right]^2}{\sum_{j,k}\sum E_{tot}^{n\,4}(j,k)}, \qquad (2)$$

where E_{tot} represents the total electric field, n is the time step of solving the forward problem, (j,k) are the grid cell coordinates, and summation is taken over the portion of the grid that represents the tissue.

III. PROPOSED MICROWAVE IMAGING SYSTEM

To examine performance of the proposed algorithm in an example, a new simple measurement setup for potential application in breast cancer detection is introduced. In most of the previous researches a multi-antenna configuration along with a multiport RF switch is used for acquiring the required data [1, 20, 31]. Here, to reduce the cost and complexity of the measurement setup we use a two antenna scanning system to replace a 12-antenna configuration. This method also reduces the undesired mutual couplings between the antennas.

For acquiring the same data as in a multi-antenna configuration, first, the transmitter is fixed and the receiver antenna scans the defined space at the specified steps. Next, the transmitter moves one step forward and

the receiver scans the remaining locations. This process is continued until the transmitter antenna completes scanning of the specified path. Because of the hemisphere shape a circular scanning path is assumed around the tissue under investigation. Selected angular step is 30º and in each scan 12 signals are recorded. It is worth mentioning that the returned signal to the transmitting antenna is also measured, that is a total of 144 measurements will be recorded. The received signals are recorded and saved for preprocessing as explained below, but before that let us consider the practical challenges encountered in this imaging system.

The main challenge is the unwanted signals which are received by the receiver antenna in addition to the signal that comes from the tumor. These signals can be categorized into three main groups. First are the unwanted signals due to the line of sight path between the transmitter and the receiver. Second is the reflected signals from the breast skin, and the last unwanted signal is due to the multipath reflections from clutter sources in tissue media.

The line of sight unwanted signals dominate the possible tumor signals, causing the failure of the imaging process. To eliminate these signals, a calibration process is employed. In this process, first in the absence of the object (here the breast tissue) all received signals are measured and saved. This calibration data is subtracted from the signals measured in the presences of the object.

For removing the effect of reflected signals from the breast skin, we first take the average of the signals received by those receivers which have the same distance and angle to the transmitter. Assuming that the skin is symmetric, by subtracting the average signal corresponding to the same distance and angle between the transmitter and receiver- from the received signal, we are able to elicit the main signal.

It is shown that the last unwanted signals due to multipath reflections in tissue media are useful for resolution improvement in TR [32].

To achieve a better resolution enabling the detection of small tumors, high frequency components should be applied. On the other hand for increasing the penetration depth to detect deep tumors in a tissue, low frequency components are required.

For these reasons UWB imaging is a good choice. Excitation signal is a Gaussian modulated signal with the standard UWB frequency band of 3.1-10.6 GHz in which acceptable contrast between malignant and normal tissues is observed [33].

Vivaldi antenna of Fig. 3 which was designed and fabricated for the experimental setup of the system explained in Section V was also used in simulations for transmitting waves to the medium and receiving signals from the tissue. Figure 4 shows the variations of the antenna VSWR and gain over the working frequency band computed by using CST Microwave Studio [34].
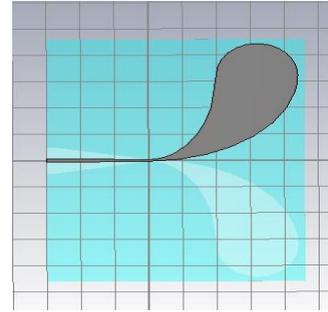

Fig. 3. Vivaldi antenna used in the proposed UWB imaging, each side of the square divisions is 1 cm.
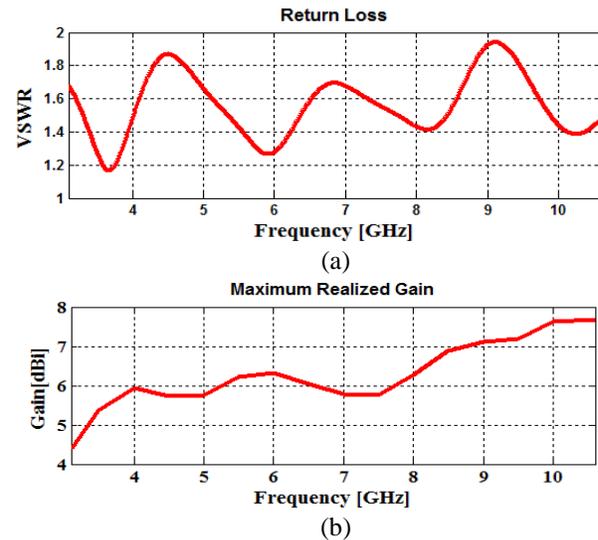

(a)

(b)

Fig. 4. Simulated (a) VSWR and (b) maximum gain of the UWB antenna.

IV. IMAGE RECONSTRUCTION SIMULATION

In this section, simulation process and simulated models for verification of the proposed algorithms are introduced. To obtain the simulated signals in time-domain, the forward problem is solved by using CST Microwave Studio software and its transient solver. Figure 5 shows the simulation environment for the two antenna configuration in the presence of the breast tissue and a typical tumor.

Discrete ports for excitation of transmitter antenna and capturing the backscattered signals in receiver are used. To simulate the breast tissue, a homogenous hemisphere with relative permittivity of 10 and radius of 10 cm is used as the simplest model. Tumor is modeled by a dielectric sphere with relative permittivity of 25 and the radius of 0.1 cm located at the coordinates (1 cm, 1 cm). Also, for modeling the skin a symmetric thin layer with thickness of 0.2 cm and relative permittivity of 35 is considered. This simple configuration permits fast and

easy data acquisitions for the 144 signals required in the data acquisition step of the proposed imaging system.

After acquiring the time domain signals, the TR signals are constructed by following the algorithm discussed before. Then these signals are fed back to the 12 antennas shown in the reconstruction configuration of Fig. 6. Again the CST Microwave Studio package is employed to solve the new forward problem at hand.
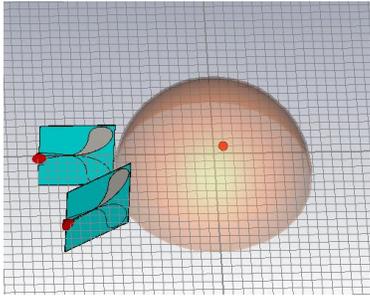

Fig. 5. A simple model for the breast tissue with one tumor used in the data acquisition process.
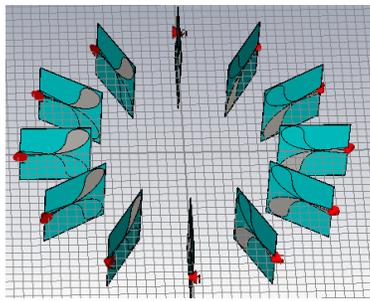

Fig. 6. Configuration of the image reconstruction process.

Since there is just one scatterer in the tissue, the conventional TR method can produce an accurate image of the tumor as shown in Fig. 7. We have used the calibration techniques introduced in Section II for removing the line of sight and skin reflections. As can be seen the tumor is well diagnosed and peak of the intensity is located exactly at the center of the tumor.

To validate the proposed modified DORT method a clutter is added to the tissue in the previous model. First two equi-radius spheres are considered at the (2 cm, 4 cm) and (-2 cm, -5 cm) locations. Dielectric properties for the tissue, skin and tumor is the same as before and clutter is considered to be caused by a relative permittivity similar to the tumor. In this situation skin reflections and the line of sight signals are omitted by using the calibration method introduced in Section II. Fig. 8 shows that the proposed modified DORT can selectively reconstruct the images of the spheres.

To examine the capability of the proposed algorithm to detect non-dominant scatterers, two spheres with the same dielectric constants but different radii are considered. One scatterer has the radius of 1.5cm and is located at (2cm, 4cm), and the other scatterer has the radius of 0.5m and is located at (-2 cm, -5 cm). As can be seen in Fig. 9, despite of having dominant scatterer, both scatterers are detected and localized with small errors.
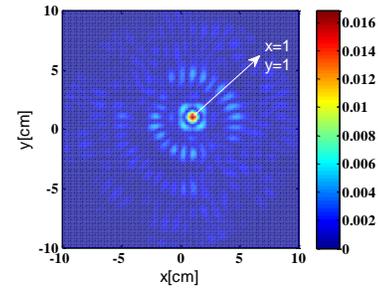

Fig. 7. The reconstructed image of the tumor by using the conventional TR method.
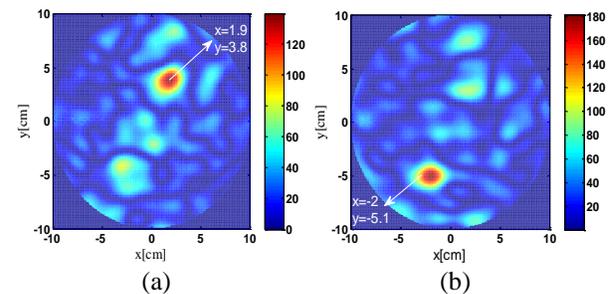

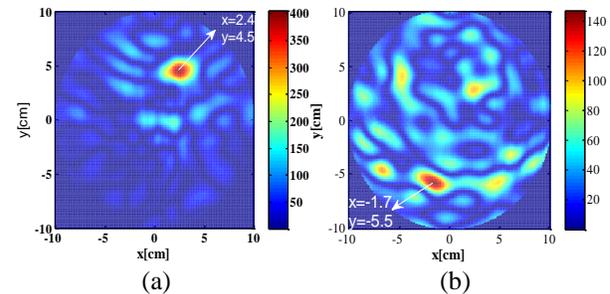Fig. 8. The reconstructed images of two equi-radius spheres located at: (a) (2, 4), and (b) (-2,-5) coordinates.

Fig. 9. Reconstructed images of two spheres with different radii of 1.5 cm and 5 mm located respectively at: (a) (2, 4) and (b) (-2, -5) coordinates.

V. EXPERIMENTAL VALIDATION

In this section, the data collected by an experimental setup of the proposed two-antenna system is used to reconstruct an object by employing the proposed algorithm. Figure 10 shows the experimental setup that has been used for this purpose. In order to demonstrate the ability of the proposed setup for detection of

scatterers, two test tubes filled with pure liquid propanol are used as detection targets. These two tubes are placed at (-2,4) and (3.5,-4) coordinates with different heights of 22 cm and 16 cm and different radii of 0.5 and 0.75 cm, respectively. The two Vivaldi antennas shown in the

Fig. 10 (a) have been used to take 64 signals at 8 locations 45° apart as explained in Section III. Here we have seven angular separations between the transmitting and the receiving antennas, at each separation the two antennas are fixed and the objects are rotated in 45° intervals by using a positioning platform, and this process is repeated for each angular separation. The angular accuracy of the positioner which is controlled by a computer is ±1° which is considered to be very coarse compared to the modern positioning systems.

First, we used a commercial UWB transceiver, i.e., TIME DOMAIN®PulsON 220, which generates and captures UWB pulses in the 3.1-6.3 GHz frequency range. In other words, this instrument has a UWB bandwidth of 3.2 GHz instead of the standard 7.5 GHz bandwidth (from 3.1 to 10.6 GHz) used in the previous section. Figure 10 (b) and Fig. 10 (c) show the reconstructed images by using the proposed method. It is clear that the two rods could be detected with reasonable accuracy.

To show the full capacity of the proposed UWB imaging system when the whole 3.1-10.6 GHz frequency band is harvested, since we could not find a commercial instrument with this specifications we designed a frequency domain measurement setup to take the required time domain data. In this experiment we employed a vector network analyzer to measure the S21 parameters of the two antennas in each location for the 1024 frequency points in the desired frequency band.

The spectrum of the desired time domain signal is then calculated by taking the product of S21 values with the spectrum of the input Gaussian excitation signal. Finally the desired UWB output signals are obtained by using IFFT. Figure 10 (d) and 10 (e) show the reconstructed images by using this setup. It is clear that more accurate images are obtained by harvesting the whole UWB frequency band; therefore it is expected that the same quality of images achieved by employing a simple UWB transceiver provided that it can use the whole 3.1-10.6 GHz UWB band.
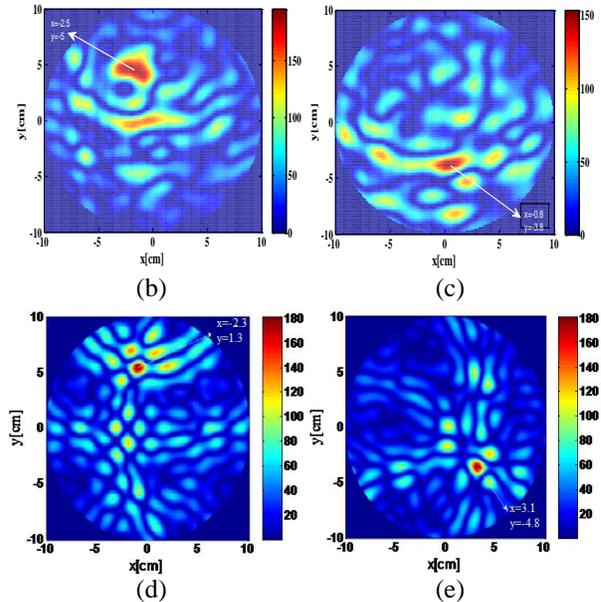

(a)

Fig. 10. (a) Experimental setup used to validate the proposed imaging system and the reconstructed images of the two tubes located at (b), (d) (-2,4) and (c), (e) (3.5, -4) coordinates first by a UWB transceiver (3.1-6.3 GHz frequency band), and then by using a Vector Network Analyzer (3.1-10.6 GHz frequency band).

VI. CONCLUSION

In this paper a TR approach for microwave imaging using UWB signals is introduced. In this approach DORT has been applied for selective focusing on multiple scatterers. A simple and cost effective imaging system has been proposed for detecting tumor-like objects using just two UWB scanning antennas and a UWB transceiver. By improving the TR algorithm, simulation results illustrates that a 1mm diameter object in a homogenous media can be detected.

The DORT algorithm is then modified to enhance itseffectiveness in detecting a non-dominant scatterer in presence of a dominant one. To implement the imaging system, two experimental setups performing in time and frequency domains, respectively, are designed. The performance of these setups to resolve two dielectric rods with different dimensions placed in a homogeneous medium are compared. It is shown that using wider frequency bands results in higher resolution as well as lower ambiguity in detecting targets. Due to the generality of the proposed imaging system, it can be used in a wide range of applications such as breast cancer recognition as well as tumor detection.

Although we considered a simple static configuration to show the effectiveness of our proposed imaging system, comprehensive clinical studies should be carried out on any medical imaging system to study its behavior in a practical dynamic situation. It is however our

expectation that the ease and speed of the data acquisition process in our proposed system can contribute to its success in the real clinical tests.

REFERENCES

[1] G. L. Charvat, L. C. Kempel, E. J. Rothwell, C. M. Coleman, and E. L. Mokole, "A through-dielectric radar imaging system," *IEEE Transactions on Antennas and Propagation*, vol. 58, no. 8, pp. 2594-2603, Aug. 2010.

[2] J. T. Case, M. T. Ghasr, and R. Zoughi, "Nonuniform manual scanning for rapid microwave nondestructive evaluation imaging," *IEEE Transactions on Instrumentation and Measurement*, vol. 62, no. 5, pp. 1250-1258, May 2013.

[3] G. S. Smith and L. E. R. Petersson, "On the use of evanescent electromagnetic waves in the detection and identification of objects buried in lossy soil," *IEEE Transactions on Antennas and Propagation*, vol. 48, no. 9, pp. 1295-1300, 2000.

[4] L. Abboud, A. Cozza, and L. Pichon, "A noniterative method for locating soft faults in complex wire networks," *IEEE Transactions on Vehicular Technology*, vol. 62, no. 3, pp. 1010-1019, Mar. 2013.

[5] J. D. Shea, B. D. Van Veen, and S. C. Hagness, "A TSVD analysis of microwave inverse scattering for breast imaging," *IEEE Transactions on Bio-medical Engineering*, vol. 59, no. 4, pp. 936-45, Apr. 2012.

[6] Y. Chen and P. Kosmas, "Detection and localization of tissue malignancy using contrast-enhanced microwave imaging: Exploring information theoretic criteria," *IEEE Transactions on Bio-medical Engineering*, vol. 59, no. 3, pp. 766-76, Mar. 2012.

[7] S. M. Aguilar, M. A. Al-Joumayly, M. J. Burfeindt, N. Behdad, and S. C. Hagness, "Multi-band miniaturized patch antennas for a compact, shielded microwave breast imaging array," *IEEE Transactions on Antennas and Propagation*, vol. 62, no. 3, pp. 1221-1231, Dec. 2013.

[8] E. J. Bond, S. C. Hagness, and B. D. Van Veen, "Microwave imaging via space-time beamforming for early detection of breast cancer," *IEEE Transactions on Antennas and Propagation*, vol. 51, no. 8, pp. 1690-1705, Aug. 2003.

[9] E. J. Bond, B. D. Van Veen, and S. C. Hagness, "An overview of ultra-wideband microwave imaging via space-time beamforming for early-stage breast-cancer detection," *IEEE Antennas and Propagation Magazine*, vol. 47, no. 1, pp. 19-34, Feb. 2005.

[10] X. Li, S. K. Davis, S. Member, S. C. Hagness, D. W. Van Der Weide, and B. D. Van Veen, "Microwave imaging via space–time beamforming: Experimental investigation of tumor detection in

multilayer breast phantoms," vol. 52, no. 8, pp. 1856-1865, 2004.

[11] Y. Xie, B. Guo, L. Xu, J. Li, and P. Stoica, "Multistatic adaptive microwave imaging for early breast cancer detection," *IEEE Transactions on Bio-medical Engineering*, vol. 53, no. 8, pp. 1647-57, Aug. 2006.

[12] F.-C. Chen and W. C. Chew, "Time-domain ultra-wideband microwave imaging radar system," *Journal of Electromagnetic Waves and Applications*, vol. 17, no. 2, pp. 313-331, 2003.

[13] M. Fink, D. Cassereau, A. Derode, C. Prada, P. Roux, and M. Tanter, "Time-reversed acoustics," *Rep. Prog. Phys.*, vol. 63, pp. 1933-1955, 2000.

[14] M. E. Yavuz and F. L. Teixeira, "Full time-domain DORT for ultrawideband electromagnetic fields in dispersive, random inhomogeneous media," *IEEE Transactions on Antennas and Propagation*, vol. 54, no. 8, pp. 2305-2315, Aug. 2006.

[15] C. Prada and M. Fink, "Eigenmodes of the time reversal operator: A solution to selective focusing in multiple-target media," *Wave Motion*, vol. 20, no. 2, pp. 151-163, Sep. 1994.

[16] M. E. Yavuz and F. L. Teixeira, "Space–frequency ultrawideband time-reversal imaging," *IEEE Transactions on Geoscience and Remote Sensing*, vol. 46, no. 4, pp. 1115-1124, Apr. 2008.

[17] J. G. Berryman, L. Borcea, G. C. Papanicolaou, and C. Tsogka, "Statistically stable ultrasonic imaging in random media," *The Journal of the Acoustical Society of America*, vol. 112, no. 4, pp. 1509, 2002.

[18] X.-M. Zhong, C. Liao, W.-B. Lin, H.-Y. Li, and H.-J. Zhou, "Time-reversal imaging based on the space-frequency MDM and cancellation operator," *Journal of Electromagnetic Waves and Applications*, vol. 28, no. 3, pp. 265-274, 2014.

[19] G. L. Charvat, L. C. Kempel, E. J. Rothwell, C. M. Coleman, and E. L. Mokole, "A through-dielectric ultrawideband (UWB) switched-antenna-array radar imaging system," *IEEE Transactions on Antennas and Propagation*, vol. 60, no. 11, pp. 5495-5500, Nov. 2012.

[20] N. Ghavami, G. Tiberi, D. J. Edwards, and A. Monorchio, "UWB microwave imaging of objects with canonical shape," *IEEE Transactions on Antennas and Propagation*, vol. 60, no. 1, pp. 231-239, Jan. 2012.

[21] L. Bellomo, M. Saillard, S. Pioch, K. Belkebir, and P. Chaumet, "An ultrawideband time reversal-based RADAR for microwave-range imaging in cluttered media," in *Proceedings of the XIII Internarional Conference on Ground Penetrating Radar*, pp. 1-5, 2010.

[22] M. Zhou, X. Chen, L. Li, and C. Parini, "The UWB imaging system with rotating antenna array for

concealed metallic object," in *EUCAP*, no. EuCAP, pp. 117-119, 2014.

[23] M. E. Yavuz and F. L. Teixeira, "Effects of array restriction on time-reversal methods," in *2007 IEEE Antennas and Propagation International Symposium*, pp. 405-408, 2007.

[24] M. E. Yavuz and F. L. Teixeira, "On the sensitivity of time-reversal imaging techniques to model perturbations," *IEEE Transactions on Antennas and Propagation*, vol. 56, no. 3, pp. 834-843, Mar. 2008.

[25] D. H. Chambers and J. G. Berryman, "Analysis of the time-reversal operator for a small spherical scatterer in an electromagnetic field," *IEEE Transactions on Antennas and Propagation*, vol. 52, no. 7, pp. 1729-1738, Jul. 2004.

[26] G. Micolau, M. Saillard, and P. Borderies, "DORT method as applied to ultrawideband signals for detection of buried objects," *IEEE Transactions on Geoscience and Remote Sensing*, vol. 41, no. 8, pp. 1813-1820, Aug. 2003.

[27] M. E. Yavuz and F. L. Teixeira, "Space-frequency ultrawideband time-reversal Imaging method as applied to subsurface objects," in *IGARSS 2008 - 2008 IEEE International Geoscience and Remote Sensing Symposium*, no. 1, pp. III – 12– III – 15, 2008.

[28] X. Xu, S. Member, E. L. Miller, C. M. Rappaport, and S. Member, "Minimum entropy regularization in frequency-wavenumber migration to localize subsurface objects," vol. 41, no. 8, pp. 1804-1812, 2003.

[29] P. Kosmas and C. M. Rappaport, "Time reversal with the FDTD method for microwave breast cancer detection," *IEEE Transactions on Microwave Theory and Techniques*, vol. 53, no. 7, pp. 2317-2323, Jul. 2005.

[30] P. Kosmas and C. M. Rappaport, "A matched-filter FDTD-based time reversal approach for microwave breast cancer detection," *IEEE Transactions on Antennas and Propagation*, vol. 54, no. 4, pp. 1257-1264, Apr. 2006.

[31] B. J. Mohammed, D. Ireland, and A. M. Abbosh, "Experimental investigations into detection of breast tumour using microwave system with planar array," *IET Microwaves, Antennas & Propagation*, vol. 6, no. 12, pp. 1311, 2012.

[32] M. E. Yavuz, "Time Reversal Based Signal Processing Techniques for Ultrawideband Electro-magnetic Sensnig in Random Media," Ohio State University, 2008.

[33] S. S. Chaudhury, R. K. Mishra, A. Swarup, and J. M. Thomas, "Dielectric properties of normal and malignant human breast tissues at radiowave and microwave frequencies," *Ind. J. Biochem. Biophys*, vol. 21, pp. 76-79, 1984.

[34] A. Mehdipour, "Antenna for ultra wideband applications," PIER, vol. 77, pp. 85-96, 2007.